frontiers | Frontiers in Earth Science

ORIGINAL RESEARCH
published: 05 May 2022
doi: 10.3389/feart.2022.874881

Geochemical Characteristics and Quality Appraisal of Groundwater From Huatugou of the Qaidam Basin on the Tibetan Plateau

Shengbin Wang[1,2], Zhan Xie[3], Fenglin Wang[1,2], Yuqing Zhang[3], Wanping Wang[1,2], Kui Liu[3], Zexue Qi[1,2], Fengyun Zhao[3], Guoqiang Zhang[1,2] and Yong Xiao[3]**

[1]Bureau of Qinghai Environmental Geological Prospecting, Xi'ning, China, [2]Key Lab of Geo-Environment of Qinghai Province, Xi'ning, China, [3]Faculty of Geosciences and Environmental Engineering, Southwest Jiaotong University, Chengdu, China

Groundwater is the foremost water resource for various purposes in arid regions. The extremely arid climate makes groundwater geochemistry there evolve faster in a short distance and water supply face higher pressure of poor geochemical quality. A hyper-arid watershed on the Tibetan Plateau was investigated to get insights into the geochemical signature, formation, and quality suitability of groundwater there. A total of 13 surface water samples and 32 phreatic groundwater samples were collected for hydrogeochemical analysis. The results showed groundwater had better hydrogeochemical quality than surface water and was more favorable for human society utilization. Groundwater was dominated by relatively fresh hydrochemical facies of HCO_3–Ca, mixed HCO_3–Na·Ca, and mixed Cl–Mg·Ca type with more than 93% of samples having the TDS below 1,000 mg/L. Most of the groundwaters were soft fresh water (84.38%) and had excellent to good quality (93%) for domestic purposes based on entropy-weighted water quality index evaluation. Groundwater was suitable for irrigation in terms of sodium and permeability hazard, but the potential salinity hazard should be concerned. The poor geochemical quality of groundwater was ascribed to the salinity caused by strong evaporation. Natural rock–water interactions including silicate weathering, carbonate dissolution, and cation exchange were still the predominated processes governing groundwater chemical composition. The influence of human activities was very limited. Groundwater resource exploitation and management should mainly consider the salinity and strong evaporation due to shallow water depth.

Keywords: hydrochemistry, salinity, groundwater quality, EWQI, arid region

OPEN ACCESS

Edited by:
Xiangjun Pei,
Chengdu University of Technology, China

Reviewed by:
Qian Sun,
Qilu University of Technology (Shandong Academy of Sciences), China
Yizhi Sheng,
Miami University, United States

****Correspondence:***
Zexue Qi
qzx13639722055@126.com
Yong Xiao
xiaoyong@swjtu.edu.cn

Specialty section:
This article was submitted to Geohazards and Georisks, a section of the journal Frontiers in Earth Science

Received: *13 February 2022*
Accepted: *04 April 2022*
Published: *05 May 2022*

Citation:
Wang S, Xie Z, Wang F, Zhang Y, Wang W, Liu K, Qi Z, Zhao F, Zhang G and Xiao Y (2022) Geochemical Characteristics and Quality Appraisal of Groundwater From Huatugou of the Qaidam Basin on the Tibetan Plateau. Front. Earth Sci. 10:874881. doi: 10.3389/feart.2022.874881

1 INTRODUCTION

Water resources are significantly important for the development of various aspects, such as human society, eco-environment, and agriculture, for a region (Gu et al., 2017b; Hao et al., 2018; Chaudhry and Sachdeva, 2020; Singh et al., 2020; Xiao et al., 2022b). Due to the scarce precipitation and surface water resource, arid and semiarid regions have more fragile eco-environment system and face greater challenges in balancing current development and sustainability when compared with humid regions (Zhang Q. et al., 2021; Li et al., 2021; Qu et al., 2021). Groundwater is essential for the development of diverse aspects of human society including domestic, irrigational, and industrial usages and also the

maintenance of the eco-environment in these water-scarce regions due to its widespread distribution, easy accessibility, and good stability (Xiao et al., 2018; Yousefi et al., 2018; Li et al., 2020; Yin et al., 2020). Thus, a comprehensive understanding of groundwater resources and their availability is crucial for the effective management of the precious water resources and sustainable development of the human community (Su et al., 2020; Dragon, 2021; Zhang J. et al., 2022).

In the past decades, research articles mainly focused on the water quantity (Hao et al., 2014; Havril et al., 2018; Omar et al., 2020). A large amount of studies were conducted to investigate the aquifer distribution and hydrogeological conditions, evaluate the quantity and sustainability of groundwater resources, and further make management policies and exploitation strategies (Gu et al., 2017b; Yin et al., 2017; Hao et al., 2018; Sun et al., 2019). In fact, groundwater availability is not only determined by the quantity but also constrained by the hydrochemical quality (Satheeskumar et al., 2020; Xiao et al., 2021b). The hydrochemical composition is the key factor determining the suitability of groundwater resources for domestic usage, industry, agriculture, and ecosystem development. Therefore, many scholars have conducted studies on groundwater chemistry regarding its status, genetic mechanisms, influencing factors, evolution, quality suitability, and so on and have made great contributions to the sustainable groundwater management worldwide (Huang et al., 2018; Yin et al., 2019; Banadkooki et al., 2020; Jiang et al., 2022).

In nature, the physicochemical composition of groundwater is governed by multiple factors including recharge water, aquifers' lithologies, residence time, and climatic conditions (Helena et al., 2000; Venkatramanan et al., 2017; Wu et al., 2020; Xiao et al., 2022a). Generally, groundwater chemistry evolves very slowly and keeps similar chemical composition (Zhang et al., 2021c), especially in humid regions. This is ascribed to the slow rock–water interaction and large recharge water quantity of humid regions. Thus, groundwater in humid regions usually presents in fresh, stable hydrogeochemical nature, and relatively good quality regionally (Zhang et al., 2021b). However, the extremely arid climatic conditions and strong evaporation in arid and hyper-arid regions make the hydrogeochemical evolution of groundwater there faster (Xiao et al., 2017; Yang et al., 2018; Zhao et al., 2018; Guo et al., 2019) and evolving from fresh water to hyper salt water even at a very short distance (Sheng et al., 2018; Luo et al., 2021). Recent drastic climate change forms new disturbance to groundwater chemistry and makes it more complex (Ma et al., 2019; Barbieri et al., 2021; Chen et al., 2021). In addition to the natural factors, groundwater chemistry has been facing the threats from human society (Guo et al., 2022). Groundwater chemistry genetic formation becomes more complex and unstable under the conditions of drastic natural climate change and great pressures of social development (Díaz-Alcaide and Martínez-Santos, 2019; Eslami et al., 2019; Yousefi et al., 2019; Zhang L. et al., 2022). Therefore, a comprehensive and deep understanding of groundwater chemistry is essential for the rational groundwater exploitation and sustainable management of groundwater resources in arid and semiarid regions.

The present study took a hyper-arid watershed in the Qaidam Basin on the Tibetan Plateau as an example to reveal the hydrogeochemical characteristics, quality, suitability, and genetic formation of groundwater in hyper-arid regions. The specific aims are to 1) illustrate and compare the hydrogeochemical signatures of surface water and groundwater, 2) understand why the groundwater resource is more suitable as the supplying water resource for arid regions, 3) assess groundwater quality for domestic and irrigation purposes, and 4) reveal the hydrogeochemical patterns of groundwater in hyper-arid regions. This research can provide scientific hydrogeochemical support for rational and sustainable utilizing groundwater in arid regions.

2 STUDY AREA

The present study area is a typical endorheic watershed located in the northwest of the Qaidam Basin on the Tibetan Plateau (**Figure 1**). It extends from 89°51′23″ to 90°47′44″ longitudes and 37°50′41″ to 38°22′4″ latitudes, and covers about 4,511 km^2 in total. This region is surrounded by the Qimantage Mountain in the south and Ahadi Mountain in the north. The Sibalik River is the main river running from the mountainous area in the southwest toward the northeast and then the east. The present study area belongs to the continental plateau climate and is characterized by strong evaporation and low rainfall. The annual average rainfall only approximates 55 mm, but the annual average evaporation can reach to about 2,850 mm. This climate feature makes the study area having scarce water resources, especially for surface water. Most water resources originate from the melting of snow and precipitation in the mountainous area.

The landform here involves the alluvial fan Gobi desert, overflow zone, and tail lake zone. Due to the shallow groundwater level, the overflow zone is presented as the desert oasis. The local resident settlements and farmlands are mainly located in this area. The lithology varies from a single thick layer of coarse-grained pebbly gravel and sand in the upper reaches area to multiple thin layers of fine sand, silt, and clay in the lower reach area (**Figure 2**). Groundwater in the basin is recharged mainly from the upper part of the alluvial fan by the Sibalik River, and flows from the southwest to the northwest and then to the east. Groundwater level depth varies from more than 100 m in the upper area to nearly 0 m in the downstream area. It discharges mainly through spring and evaporation.

3 MATERIAL AND METHODS

3.1 Sampling and Analysis

A total of 13 surface water samples and 32 groundwater samples were collected from the study area. The surface waters were mainly sampled from the rivers from the mountain pass to the Lake Gas Hure. Groundwater samples were concentrated in the middle reaches of the watershed where the human settlements and farmlands were located. All groundwaters were sampled from the phreatic aquifers. All samples were collected during the summer of 2020. The samples were collected in pre-washed

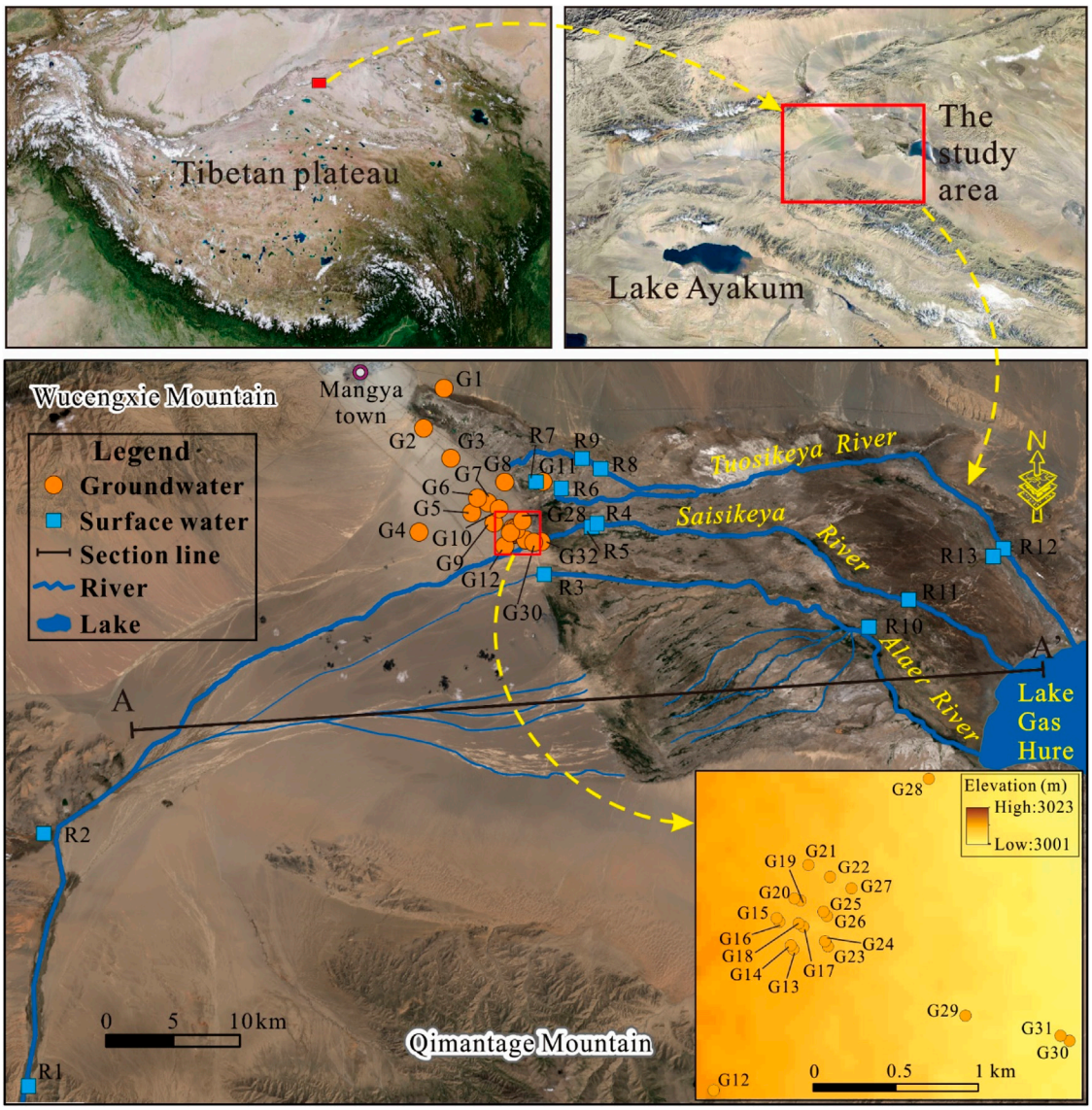

FIGURE 1 | Location map of the Hutugou watershed and groundwater sampling points.

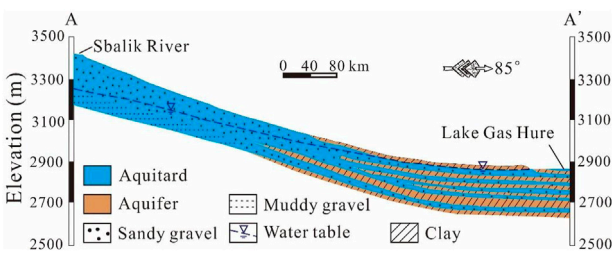

FIGURE 2 | Cross section presenting hydrogeological condition along the A-A'.

high-density polyethylene bottles with 1-L volume. Groundwater was sampled from boreholes and wells after pumping for more than 15 min. The samples were stored under 4°C and sent to the laboratory of groundwater sciences and engineering of the institute of hydrogeology and environmental geology, Chinese Academy of Geological Sciences for analysis within 24 h. Parameters including water temperature (T), pH, and electrical conductivity (EC) were measured *in situ* using a portable instrument (HANNA HI98130, Italy). Other parameters were determined in the laboratory. The HCO_3^- was determined using acid–base titration. Ions including Cl^-, SO_4^{2-}, NO_3^-, NO_2^-, NH_4^+, and F^- were measured with the aid of ion chromatography (Shimadzu LC-10ADvp, Kyoto, Japan). Major cations involving K^+, Na^+, Ca^{2+}, and Mg^{2+} were determined by the inductively coupled plasma spectrometry (Agilent 7500ce ICP-MS, Tokyo, Japan). Total dissolved solids (TDS) were obtained using the gravimetric method. The accuracy of laboratory analysis was checked with the aid of ionic charge

balance error percentage (**Eq. 1**) (Xiao et al., 2022c). All samples had the ionic charge balance error percentage between -5% and 5%, indicating reasonably good analytical accuracy.

$$\%ICBE = \frac{\sum_i^m ce_i^+ - \sum_i^m ce_i^-}{\sum_i^m ce_i^+ + \sum_i^m ce_i^-}, \quad (1)$$

where ce_i^+ represents the charge concentration of a specific cation and ce_i^- is the charge concentration of a specific anion. All of them have the unite of milliequivalent per liter.

3.2 Entropy-Weighted Water Quality Index

The entropy-weighted water quality index (EWQI) is an improved comprehensive approach based on the water quality index (WQI) which is widely used to assessing the suitability of groundwater quality for domestic purposes. The EWQI assessment can be performed as follows:

Step 1: obtaining the eigenvalue matrix Y (**Eq. 2**) with the normalized physicochemical data that can be obtained *via* **Eq. 3**.

$$Y = \begin{bmatrix} y_{11} & y_{12} & \cdots & y_{1n} \\ y_{21} & y_{22} & \cdots & y_{2n} \\ \vdots & & \ddots & \vdots \\ y_{m1} & y_{m2} & \cdots & y_{mn} \end{bmatrix}, \quad (2)$$

$$y_{ij} = \frac{x_{ij} - (x_{ij})_{min}}{(x_{ij})_{max} - (x_{ij})_{min}}, \quad (3)$$

where m and n are the number of sample and index, respectively, x_{ij} signifies the value of parameter j of sample i, and$(x_{ij})_{\max}$ and $(x_{ij})_{\min}$ present the maximum and minimum of samples' parameters, respectively.

Step 2: calculating the entropy weight of each parameter.

$$P_{ij} = \frac{y_{ij}}{\sum_{i=1}^m y_{ij}}, \quad (4)$$

$$e_j = -\frac{1}{lnm} \sum_{i=1}^m (P_{ij} \times lnP_{ij}), \quad (5)$$

$$w_j = \frac{1 - e_j}{\sum_{i=1}^n (1 - e_j)}, \quad (6)$$

where P_{ij} is the ratio of parameter j of sample I, e_j signifies the information entropy of parameter j, and w_j denotes the entropy weight of parameter j.

Step 3: obtaining the quality rating scale (q_j) of every sample.

$$q_j = 100 \times \frac{C_j}{S_j}, \quad (7)$$

where C_j signifies the parameter value of each sample and S_j is the permissible limit of each parameter recommended by the national standard or World Health Organization.

Step 4: computing the EWQI value.

$$EWQI = \sum_{j=1}^m (w_j \times q_j). \quad (8)$$

The chemical quality of water can be divided into five categories based on the aforementioned EWQI value, that is, excellent quality (EWQI ≤ 50), good quality (50 < EWQI ≤ 100), medium quality (100 < EWQI ≤ 150), poor quality (150 < EWQI ≤ 200), and extremely poor quality (EWQI > 200).

4 RESULTS AND DISCUSSION

4.1 Physicochemical Features of Surface Water and Groundwater

The physicochemical characteristics of sampled surface waters and groundwaters were statistically summarized in **Table 1**. The guidelines of drinking water recommended by the Chinese guideline (GAQS, 2017) and World Health Organization (WHO, 2017) were also involved in the Table for comparison.

Surface water in the study area showed a slightly alkaline feature with the pH value varying from 7.58 to 8.84, averaging at 8.27. The total dissolved solids (TDS) of sampled surface waters in the study area ranged from 503.20 mg/L to 7,669.06 mg/L, demonstrating a significant large salinity variation feature. It averaged at 2,568.73 mg/L, and approximately 53.85% of samples exceeded the drinking water guideline of 1,000 mg/L. Surface water demonstrated relatively fresh characteristics in the middle–upper stream area, but saline features in the middle–lower stream area. This coincides with the arid climate characteristics of the study area. All the major cations and anions also showed large variations in the concentration, suggesting fresh to extremely saline features for surface water from the mountain pass to the terminal lake. The concentrations of F^- and NO_2^- of sampled surface waters were all below the detected limits. The NO_3^- and NH_4^+ were in the range of 1.00–50.00 mg/L and 0.00–0.20 mg/L, respectively, with an average of 6.85 mg/L and 0.06 mg/L. These two ions were all within the drinking water guidelines for all sampled surface waters.

Groundwater sampled in the study area had the pH value in the range of 6.97–8.89 with a mean of 7.93, indicating a nearly neutral to slightly alkaline nature. The TDS value of groundwater varied from 368.32 mg/L to 5,838.14 mg/L with a mean of 822.70 mg/L. Groundwater also showed a large variation of salinity in the study area, but was much fresher than the surface water. Approximately 93.75% of sampled groundwaters were with the TDS value below the desirable limit of 1,000 mg/L, implying good quality for drinking purposes. The concentrations of major cations and anions in groundwater presented relatively small variations when compared with surface water. The concentration of Na^++K^+ ranged from 56.30 mg/L to 641.2 mg/L with an average of 127.57 mg/L. The Ca^{2+} and Mg^{2+} concentrations of groundwater were in the range of 16.03–350.70 mg/L and 23.08–856.58 mg/L, respectively. The contents of major anions were in the range of 74.45–1,538.53 mg/L for Cl^-, 38.42–768.48 mg/L for SO_4^{2-}, and 146.45–3,356.10 mg/L for HCO_3^-. Except for the sample collected at G31, all other sampled groundwaters in the study area had relatively low major ion concentrations, indicating fresh nature. F^-, NO_3^-, and NH_4^+ of groundwater were observed with the concentration in the range of 0.00–0.08 mg/L, 0.00–24.00 mg/L and 0.00–0.12 mg/L, respectively. All groundwater samples had these three ion content below the desirable limits for drinking purposes. The concentration of NO_2^- in sampled groundwaters

TABLE 1 | Statistical \summary of the physicochemical parameters of groundwater and related guideline for drinking water purpose.

	Index	Unit	Min	Max	Mean	SD[a]	Guideline	% of samples beyond the guideline
Surface water	T	°C	4.50	16.00	8.51	3.58	—	—
	pH	—	7.58	8.84	8.27	0.32	6.5–8.5[b]	23.08%
	TH	mg/L	275.22	1989.09	948.88	702.75	450[b]	53.85%
	TDS	mg/L	503.20	7,669.06	2,568.73	2,348.87	1,000[b]	53.85%
	Na^++K^+	mg/L	73.02	2,120.31	580.82	671.86	—	—
	Ca^{2+}	mg/L	60.12	350.70	129.34	95.33	75[c]	69.23%
	Mg^{2+}	mg/L	24.30	428.29	151.97	164.08	50[c]	46.15%
	Cl^-	mg/L	120.53	3,296.85	849.85	1,045.33	250[b]	38.46%
	SO_4^{2-}	mg/L	96.06	1,431.29	648.93	527.56	250[b]	61.54%
	HCO_3^-	mg/L	42.24	646.81	341.14	197.36	—	—
	F^-	mg/L	—	—	—	—	1.0[b]	—
	NO_3^-	mg/L	1.00	50.00	6.85	13.25	50.0[c]	0%
	NO_2^-	mg/L	—	—	—	—	0.02[b]	—
	NH_4^+	mg/L	0.00	0.20	0.06	0.06	0.2[b]	0%
Groundwater	T	°C	4.00	13.00	7.37	2.40	—	
	pH	—	6.97	8.89	7.93	0.33	6.5–8.5[b]	3.13%
	TH	mg/L	155.12	4,403.52	517.20	941.90	450[b]	6.25%
	TDS	mg/L	368.32	5,838.14	822.70	1,105.75	1,000[b]	6.25%
	Na^++K^+	mg/L	56.30	641.20	127.57	114.38	—	
	Ca^{2+}	mg/L	16.03	350.70	72.96	60.80	75[c]	12.5%
	Mg^{2+}	mg/L	23.08	856.58	83.29	192.87	50[c]	9.38%
	Cl^-	mg/L	74.45	1,538.53	182.46	295.16	250[b]	6.25%
	SO_4^{2-}	mg/L	38.42	768.48	151.82	163.90	250[b]	6.25%
	HCO_3^-	mg/L	146.45	3,356.10	451.17	718.23	—	
	F^-	mg/L	0.00	0.08	0.01	0.02	1.0[b]	0%
	NO_3^-	mg/L	0.00	24.00	4.28	4.22	50.0[c]	0%
	NO_2^-	mg/L	0.00	0.24	0.02	0.05	0.02[b]	9.38%
	NH_4^+	mg/L	0.00	0.12	0.02	0.04	0.2[b]	0%

[a]*Standard deviation.*
[b]*Chinese guideline (GAQS, 2017).*
[c]*WHO guideline (WHO, 2017).*

varied between 0.00 and 0.24 mg/L with a mean of 0.02 mg/L. About 9.38% of groundwater samples (0.08 mg/L for G23 and G25, 0.24 mg/L for G31) were found with the NO_2^- content exceeding the desirable limit of 0.02 mg/L.

4.2 Hydrogeochemical Facies of Surface Water and Groundwater

The hydrogeochemical composition and features of surface water and groundwater were demonstrated using the Piper trilinear diagram (**Figure 3**). The lower left and lower right triangular of the Piper trilinear diagram demonstrate the cations and anions composition, respectively, and the diamond field in the center presents the different hydrochemical facies that water samples may belong to (Gu et al., 2017a; Gu et al., 2019; Jiang et al., 2022; Xiao et al., 2022a).

The Piper diagram showed that almost all surface water samples were plotted in the [Na^+] type field of the lower-left triangular (**Figure 3A**), suggesting that surface water in the study area was dominated by Na^+ for the cations. This coincides with the arid climatic features of the study area. While for the major anions, although most of the surface water samples were observed situating in the [Cl^-] type field of the lower-right triangular (**Figure 3A**), some surface water samples were also found plotting in the [SO_4^{2-}] and [HCO_3^-] type field. This suggests that the surface water evolved from the fresh hydrochemical facie of HCO_3^- type to salty Cl^- type in the study area. It can be seen from the central diamond shape of the Piper diagram (**Figure 3A**), the hydrochemical facies of surface water evolved from the fresh type of HCO_3–Ca to salty Cl–Na. Surface water in the study area was dominated by salty mixed Cl–Ma·Ca type and Cl–Na type, followed by fresh HCO_3–Ca type and salty Cl–Ca type. As presented in **Table 1**, more than 53% of the sampled surface waters had the TDS beyond the drinking desirable limit of 1,000 mg/L, thus, were not suitable for drinking purposes in most locations of the study area.

As demonstrated in **Figure 3B**, most of the sampled groundwaters were plotted in the [Na^+] type field of the lower-left triangular and the [HCO_3^-] type field of the lower-right triangular of the Piper diagram, suggesting Na^+ and HCO_3^- were the dominant cation and anion for groundwater in the study area. It can be seen that some groundwater samples were situating in the [Ca^{2+}] type or [Mg^{2+}] field of the lower-left triangular and in the [SO_4^{2-}] type or [Cl^-] field of the lower-right triangular of the Piper

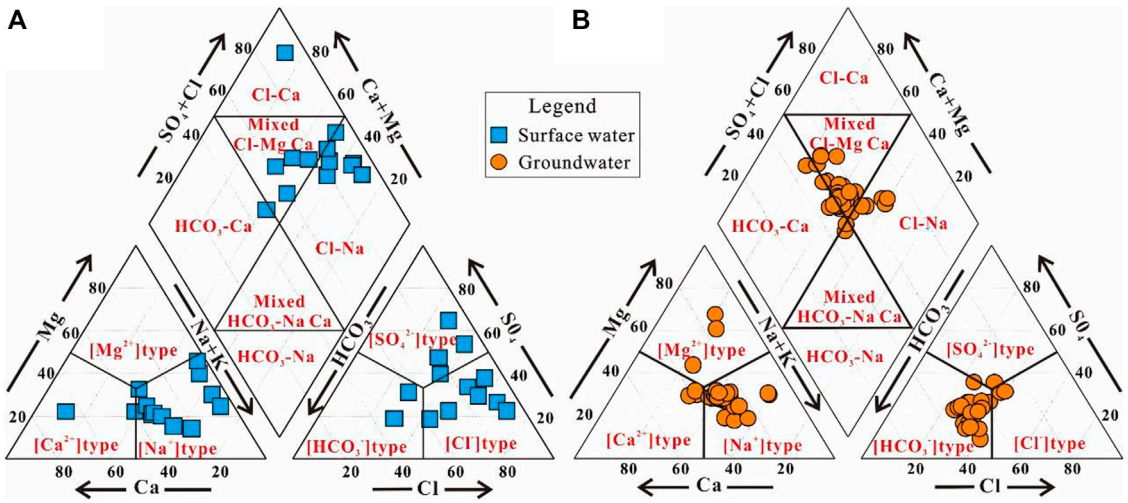

FIGURE 3 | Piper diagrams showing the hydrochemistry of **(A)** surface water and **(B)** groundwater in the study area.

diagram, illustrating that some groundwaters in the study area were dominated by Ca^{2+} or Mg^{2+} for the cations and SO_4^{2-} or Cl^- for the anions. The central diamond shape of the Piper diagram presented that the sampled groundwaters in the study area were in the hydrochemical facies of HCO_3–Ca, mixed HCO_3–Na·Ca, mixed Cl–Mg·Ca, and Cl–Na (**Figure 3B**). Most of the samples had relatively fresh hydrochemical facies, and about 15.63, 6.25, and 62.5% of the sampled groundwaters belonged to the HCO_3–Ca, mixed HCO_3–Na·Ca, and mixed Cl–Mg·Ca types, respectively. In addition, approximately 15.63% of groundwater samples were classified as the relatively salty hydrochemical facies of Cl–Na (**Figure 3B**). Groundwater in the study area also presented an evolution from a very fresh hydrochemical feature to salty hydrochemical feature. This coincides with the surface water evolution. Groundwater showed a slow evolving rate from fresh water to the salty water, and presents fresher features in the middle–upper area when compared with surface water at the same location. The statistical summary of groundwater chemical composition (**Table 1**) also suggested the sampled groundwaters had a relatively good quality in terms of the salinity. More than 93% of the sampled groundwaters were with the TDS within the drinking desirable limit of 1,000 mg/L. Thus, groundwater is the prior water resource for various purposes of the local development.

4.3 Groundwater Quality Assessment

As described previously, groundwater in the study area has fresher quality than surface water and is more favorable for various usages, thus, more attentions are paid to groundwater in the present study.

4.3.1 Domestic Purpose

The sampled groundwaters were plotted in the integrated water quality diagram of the total hardness (TH) versus the total dissolved solids (TDS) (**Figure 4**). It can be clearly seen that most of the sampled groundwaters belonged to the moderately hard fresh category (9.38%) and the soft fresh category (84.38%). Only two groundwater samples (6.25%) were observed situating in the poor quality category, and all of these two groundwater samples belonged to the very hard brackish category. Overall, groundwater in the study area had relatively good quality in terms of TH and TDS.

To further illustrate the quality of groundwater for drinking purposes, the entropy-weighted water quality index (EWQI) approach was introduced in the present study. Parameters except for water temperature (T) were all involved in the EWQI assessment. The results demonstrated that groundwater in the study area had a relatively large variation of EWQI values ranging from 22 to 461 (**Figure 5**). Most of the groundwater samples (90.63%) were with the

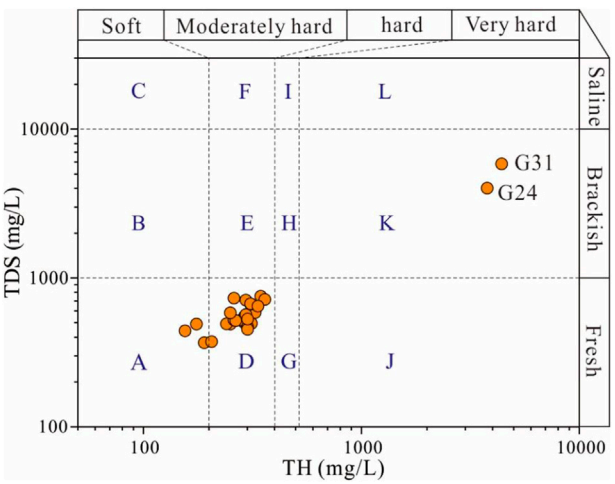

FIGURE 4 | Plots of total hardness (TH) versus total dissolved solids (TDS) of groundwater.

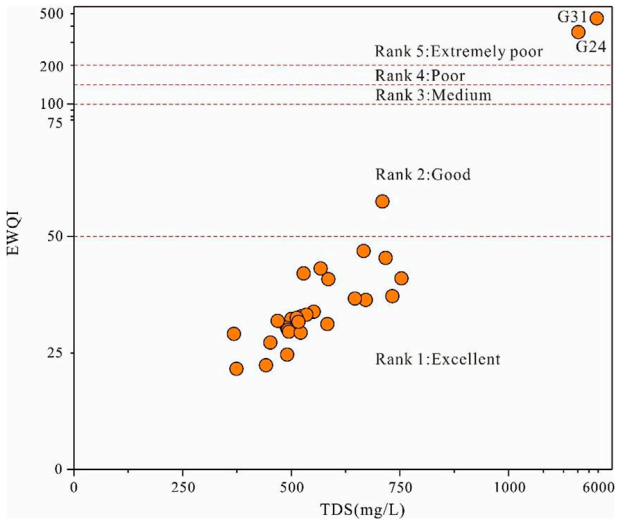

FIGURE 5 | Plots of total dissolved solids (TDS) versus EWQI value of groundwater.

EWQI value below 50, implying excellent water quality (Rank 1). In addition, one groundwater sample (3.13%) had the EWQI value in the range of 50–100 (Rank 2), indicating good water quality. All the groundwaters of these two categories were quite suitable for drinking purposes. The other two sampled groundwaters (i.e., G24 and G31) (6.25%) had a relatively high EWQI value of 357 and 461, respectively, and belonged to the extremely poor quality category (Rank 5), implying groundwater at these two sites were not suitable for direct drinking purposes. This result coincides with the aforementioned results of the integrated water quality diagram (**Figure 4**). Overall, most groundwater in the study area had relatively good quality and suitable for domestic purpose.

In particular, the EWQI value of groundwater sampled at G24 was dominantly contributed by Mg^{2+}, TH, HCO_3^-, Cl^-, SO_4^{2-}, and TDS, Ca^{2+} with the contribution percentage of 33, 17, 12, 7, 7, 7, and 5%, respectively. The groundwater sampled at G31 was predominantly contributed by Mg^{2+}, TH, NO_2^-, HCO_3^-, Cl^-, TDS, SO_4^{2-}, and Ca^{2+} with the contribution percentage of 28, 15, 13, 11, 8, 7, 6, and 6%, respectively. Therefore, the relatively poor overall quality of groundwater in the study area is predominantly ascribed to the high salinity. The high nitrite concentration is also responsible for the high EWQI value, that is , the poor quality of groundwater G31.

4.3.2 Irrigational Purpose

The high concentration of ions in irrigation water could pose irreversible harms to soil structure. Special attention should be paid to the arid and semiarid regions due to the potential high salinity of water caused by strong evaporation (Luo et al., 2021).

The sodium adsorption ratio (SAR) is an effective approach to reveal the possible soil structure damage caused by the replacement of the Ca^{2+} and Mg^{2+} on soil mediums to Na^+ in irrigation water (Xiao et al., 2021a). It is commonly coupled with the EC value to illustrate the potential sodium and salinity hazard when used for long-term irrigation. As demonstrated in **Figure 6**, except for the groundwater sampled at G31, other samples belonged to the S1 category of sodium hazard assessment, suggesting a low sodium hazard for water used for long-term irrigation usage. For groundwater sample G31, it is located in the S2 category, indicating a medium sodium hazard. For the salinity hazard, the sampled groundwaters were observed plotted in three categories including C2, C3, and C4. Groundwater samples were dominantly plotted in the C3 category (84.38%), and a small portion was situated in the C2 (6.25%) and C4 (6.25%), implying a high salinity hazard for groundwaters at most sampling sites (84.38%), and a medium hazard and very high hazard for groundwaters at a small portion of sampling sites (6.25% for medium hazard, and 6.25% very high hazard).

Percentage sodium (%Na) is a robust tool to reveal the possible hazard of Na^+ posed to the structure of soils (Xiao et al., 2020). It has been widely combined with the EC to construct the Wilcox diagram to assess the suitability of water for agricultural irrigation. As shown in **Figure 7**, most sampled groundwaters were situated in the categories of excellent to good (6.25%), good to permissible (84.38%), and permissible to suitable (3.13%), demonstrating suitable quality for agricultural irrigation. Meanwhile, two groundwater samples (G24 and G31) were found with a high sodium hazard risk if used for long-term irrigation, thus not suitable for agricultural usage.

The permeability index (PI) is a useful parameter for revealing the permeability effect posed by irrigation water and has been widely used worldwide (Xiao et al., 2020; Luo et al., 2021). The Doneen diagram, which coupled PI with the total concentration, groups the irrigation water quality into three categories, that is, class-I, class-II, and class-III (Gu et al., 2018; Xiao et al., 2021a). The class-I category indicates irrigation water would make the soil 100% maximum permeability and is suitable for long-term agricultural irrigation. The class-II and class-III categories demonstrate 75% maximum permeability and 25% maximum permeability, respectively, and are slightly appropriate and not

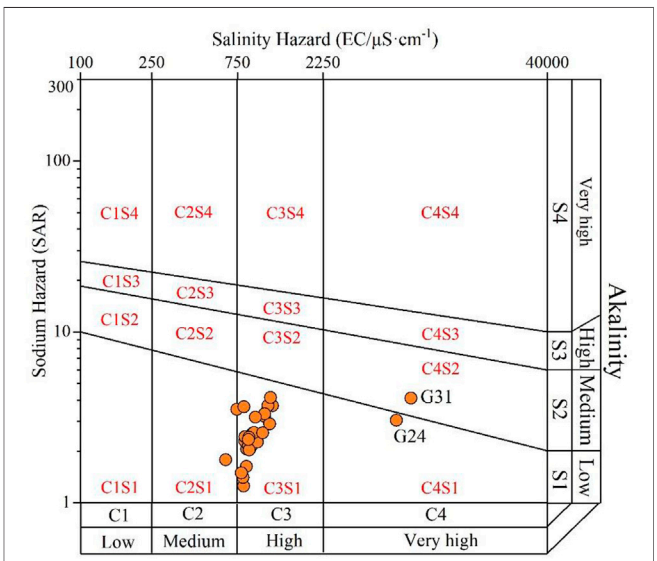

FIGURE 6 | Irrigation quality of groundwater in relation to sodium and salinity hazard.

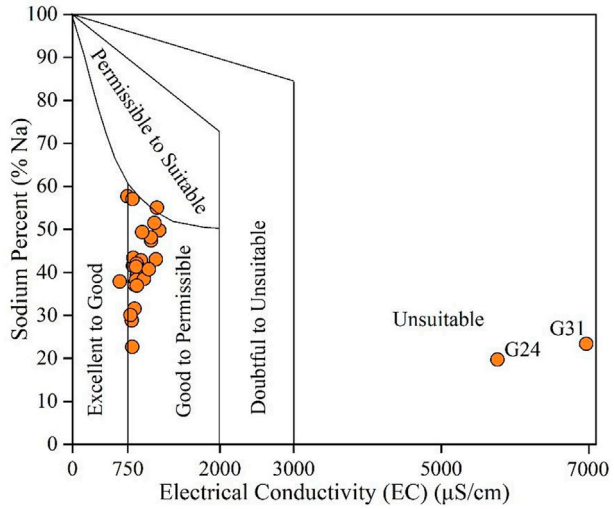

FIGURE 7 | Wilcox diagram presenting the suitability of groundwater quality for irrigation.

suitable for irrigation. The assessing results of the Doneen diagram are shown in **Figure 8**. It can be clearly seen that all sampled groundwaters had the PI value below 80, and 93.75 and 6.25% of samples belonged to class-I and class-II categories, respectively. This suggests that all groundwater sampled in the study area would not threaten the permeability of soil when used for long-term agricultural irrigation.

Overall, groundwaters sampled in the study area had nearly no sodium hazard and permeability hazard to soil structure. However, salinity hazards should be concerned as more than 93% of groundwater samples may pose high to very high salinity threats to soils if used for long-term irrigation. This mainly occurs in the lower reaches of the watershed where the groundwater level is relatively shallow.

4.4 Hydrogeochemical Patterns of Groundwater

Understanding the mechanisms governing groundwater chemical compositions is essential for rational groundwater resource exploitation and sustainable management (Hao et al., 2020).

In nature, groundwater chemistry is dominantly governed by three categories, that is, precipitation, rock–water interaction, and evaporation (Xiao et al., 2022a). These three main governing mechanisms can be visually revealed using the Gibbs diagrams that constructed by $Na^+/(Na^+{+}Ca^{2+})$ vs. TDS and $Cl^-/(Cl^- + HCO_3^-)$ vs. TDS (Hao et al., 2020). As shown in **Figure 9**, most of the groundwater samples (93.75%) were plotted in the rock dominance, illustrating that the sampled groundwaters in the study area were dominantly controlled by the rock–water interaction on the hydrochemical composition. In addition, two samples (G24 and G31) were observed plotting the evaporation dominance of the two sub-diagrams of Gibbs, suggesting that the hydrochemistry of groundwater at these two sites was mainly controlled by evaporation in nature. Thus, the poor water quality of groundwater for domestic and irrigational purposes was dominantly caused by the strong evaporation.

To further illustrate the specific rock–water interaction contributing to most of the groundwater samples, the end-member diagrams of Na^+-normalized Ca^{2+} versus HCO_3^- (Xiao et al., 2022b) of groundwater were introduced in the present study. As illustrated in **Figure 10**, groundwater samples collected in the study area were situated in the silicate dominance and toward the carbonates dominance, indicating the natural chemical components of groundwater in the study area dominantly originated from the silicate weathering (**Eq. 9**) and also carbonate dissolution. However, evaporative dissolution was not the main contributor of groundwater chemical composition.

$$2NaAlSi_3O_8{+}2CO_2{+}11H_2O{\rightarrow}Al_2Si_2O_5(OH)_4{+}4H_4SiO_4{+}2Na^+ {+}2HCO_3^-. \quad (9)$$

The bivariate plots of major chemical ions of groundwater were presented in **Figure 11**. As shown in **Figure 11A**, most of the groundwater samples were plotted away from the halite line (Na^+/Cl^- ratio of 1:1), suggesting that halite dissolution was not the main process contributing major ions to groundwater. In addition, it can be clearly seen from the **Figures 11B,C** that almost all groundwater samples were also observed situating away from the 1:1 line of Ca^{2+}/SO_4^{2-} and $(Ca^{2+}{+}Mg^{2+})/SO_4^{2-}$, indicating that the sulfate dissolution was not the main contributor of groundwater chemical composition. All the aforementioned facts confirmed the end-member results that groundwater chemistry was not controlled by evaporative dissolution. In the meantime, **Figure 11D** shows that most of the groundwater samples were plotted along the 1:1 line of $(Ca^{2+}{+}Mg^{2+})/(SO_4^{2-} + HCO_3^-)$,

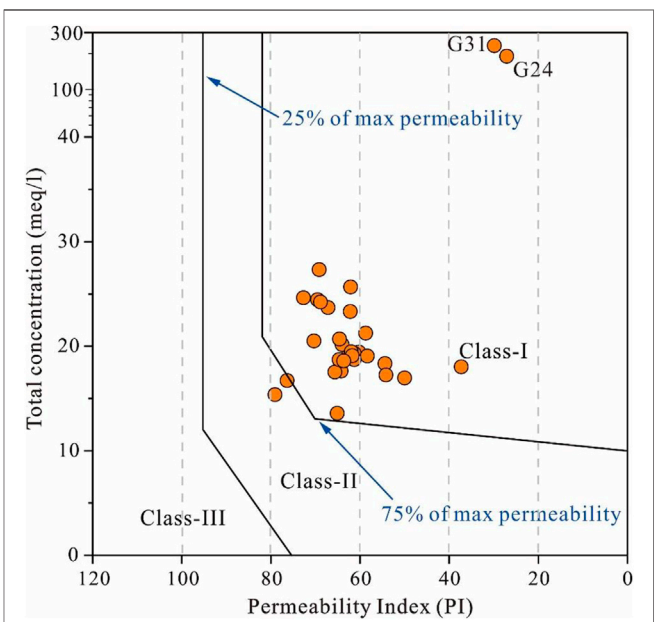

FIGURE 8 | Doneen diagram for assessing the suitability of groundwater quality for irrigation.

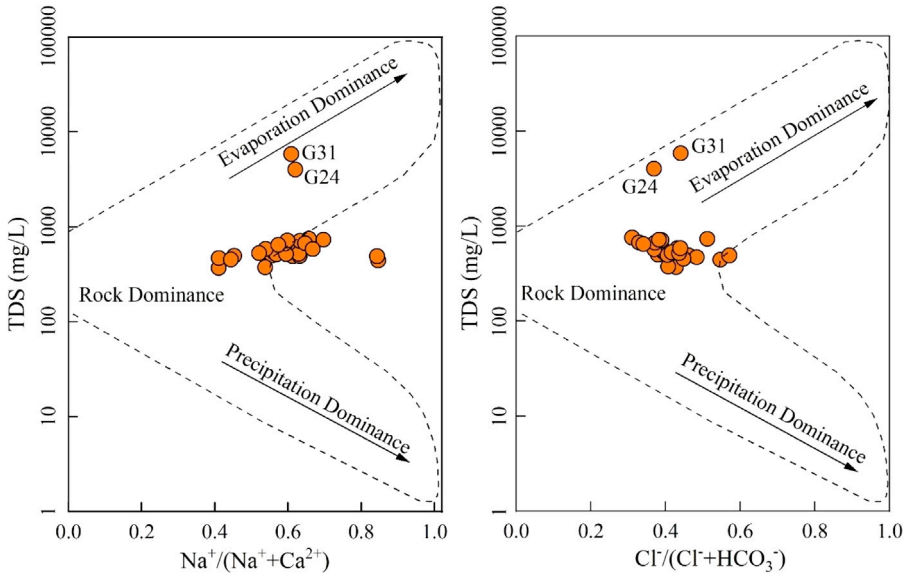

FIGURE 9 | Gibbs diagrams for groundwater samples in the study area.

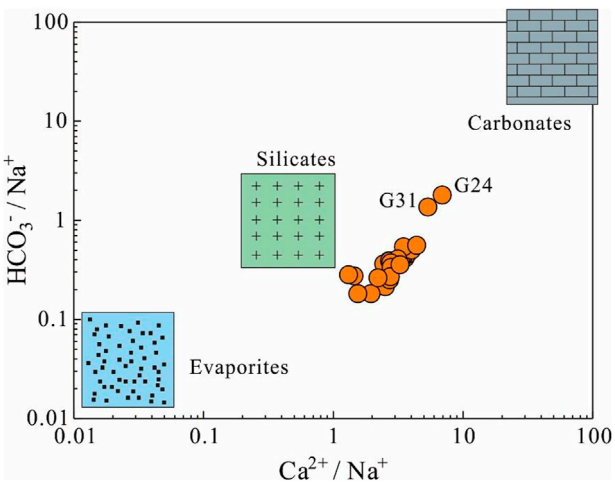

FIGURE 10 | Plots of Na-normalized Ca versus HCO_3 of groundwater in the study area.

implying sulfate dissolution or carbonate dissolution. However, as mentioned previously, the sulfate dissolution is not the main process; thus, carbonate dissolution is the process contributing to the major chemistry of groundwater in the study area. This coincides with the end-member diagram results.

In addition, ion exchange is also an important proces in the groundwater environment. Chloro-alkaline indices (CAI-1 and CAI-2) expressed in **Eqs 10** and **11** are useful tools to get insights into potential ion exchange interactions (Hao et al., 2020; Xiao et al., 2022b). As shown in the bivariate diagram of chloro-alkaline indices (**Figure 12**), most of the groundwater samples (84.38%) were with the negative CAI-1 and CAI-2, indicating the cation-exchange reaction (**Eq. 12**) is an important process contributing groundwater chemistry. This process dominantly occurs in the fresher groundwater in the upper part of the watershed. Meanwhile, about 15.63% of sampled groundwaters were observed to have positive values for both CAI-1 and CAI-2, implying the reverse cation-exchange reaction (**Eq. 13**). However, this process was dominantly situated in the lower parts of the watershed with relatively higher salinity.

$$\mathbf{CAI-1} = \frac{Cl^- - (Na^+ + K^+)}{Cl^-}, \tag{10}$$

$$CAI-2 = \frac{Cl^- - (Na^+ + K^+)}{SO_4^{2-} + CO_3^{2-} + HCO_3^- + NO_3^-}, \tag{11}$$

$$Ca^{2+}\ (\text{or } Mg^{2+}) + 2NaX\ (\text{solids}) \rightarrow 2Na^+ + CaX_2\ (\text{or } MgX_2)\ (\text{solids}), \tag{12}$$

$$2Na^+ + CaX_2\ (\text{or } MgX_2)\ (\text{solids}) \rightarrow Ca^{2+}\ (\text{or } Mg^{2+}) + 2NaX\ (\text{solids}). \tag{13}$$

Anthropogenic inputs are found to be another important contribution to groundwater chemical composition in many regions worldwide and cannot be ignored. NO_3^- is an important indicator for anthropogenic inputs into the groundwater environment. Generally, the natural background limit of NO_3^- is 10 mg/L. Groundwater with NO_3^- concentration beyond this limit is usually considered as being influenced by anthropogenic pollution inputs. In the present study, only one collected groundwater sample (G24) was found with the NO_3^- concentration of 24 mg/L and beyond this natural limit. All other groundwater samples had the NO_3^- concentration within the natural threshold. Therefore, anthropogenic pollutant inputs were not a widespread process contributing to groundwater chemistry.

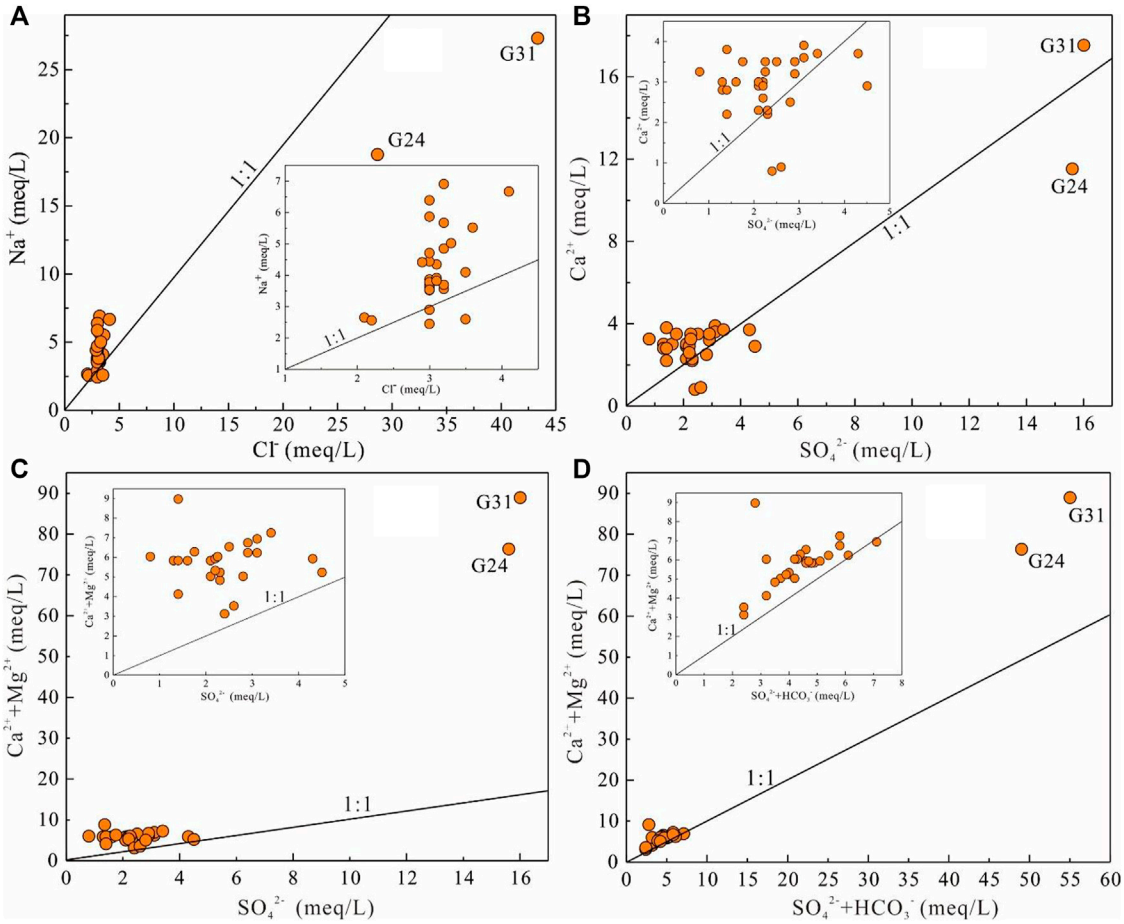

FIGURE 11 | Scatter plots of **(A)** Na^+ vs. Cl^-, **(B)** Ca^{2+} vs. SO_4^{2-}, **(C)** (Ca^{2+}+Mg^{2+}) vs. SO_4^{2-}, and **(D)** (Ca^{2+}+Mg^{2+}) vs. (SO_4^{2-} + HCO_3^-) of groundwater in the study area.

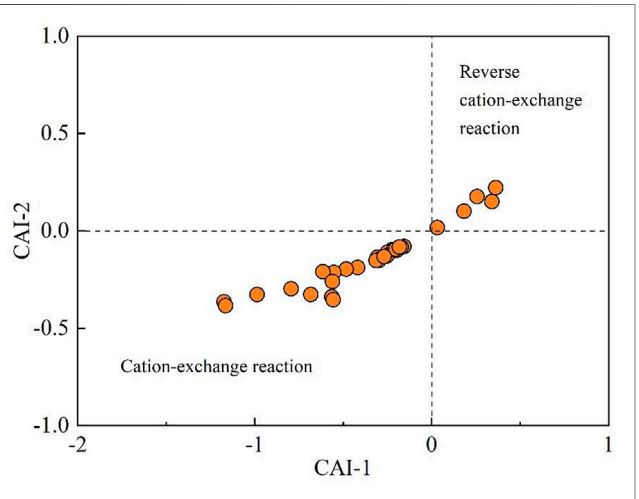

FIGURE 12 | Scatter plots of chloro-alkaline indices illustrating ion exchange reaction.

Groundwater at the local site (G24) should be concerned for the anthropogenic pollution. In addition, three sites were found with the NO_2^- concentration exceeding the drinking water desirable limit, and also implied anthropogenic influence. Fortunately, these two ions were not observed to have the significant relationships with other major ions according to the Pearson correlation coefficient results. Thus, although anthropogenic pollution inputs had elevated the content of nitrogen, the major chemistry of groundwater was not affected by anthropogenic activities. Therefore, salinity caused by strong evaporation is the main threat to groundwater quality in the study area.

5 CONCLUSION

A hyper-arid watershed in the Qaidam Basin on the Tibetan Plateau was investigated concerning its groundwater geochemical characteristics, genesis, and quality suitability. The main findings are as follows:

The present research indicated groundwater and surface water in the study area had a slightly alkaline nature and their hydrochemistry was characterized by arid climatic features. Both groundwater and surface water had a large variation of salinity and evolved from fresh water to salty water in the watershed. Surface water was dominated by salty mixed Cl–Ma·Ca type and Cl–Na type, and more than 53% of the sampled surface waters had the TDS beyond the drinking desirable limit of 1,000 mg/L. Most of the sampled groundwaters belonged to the relatively fresh hydrochemical facies of HCO_3–Ca, mixed HCO_3–Na·Ca, mixed Cl–Mg·Ca type, and less than 7% of samples had the TDS exceeding the drinking desirable limit. Groundwater had relatively good quality in terms of the salinity when compared with surface water, and was the prior water resource for the local water supply.

Groundwater in the study area was mainly soft fresh water (84.38%), followed by moderately hard fresh water (9.38%) and very hard brackish water (6.25%). The sampled groundwaters had the EWQI value ranging from 22 to 461, and more than 93% of groundwater was excellent to good quality (EWQI < 100). The poor quality of groundwater was dominantly ascribed to the salinity, and also contributed by the nitrite locally. Most of the sampled groundwaters were suitable for irrigation and would not pose a sodium hazard and permeability hazard, but the salinity hazard should be concerned.

The geochemical composition of groundwater in the study area was dominantly governed by the natural rock–water interaction. The poor quality of groundwater at local sites was ascribed to the relatively high salinity caused by strong evaporation rather than anthropogenic influence. Groundwater chemical components mainly originated from silicate weathering, carbonate dissolution, and cation exchange. Anthropogenic pollution only elevated some local nitrogen concentration, but was not responsible for the high salinity. Groundwater salinity caused by strong evaporation should be considered in groundwater exploitation and management in arid regions like the present study area.

DATA AVAILABILITY STATEMENT

The raw data supporting the conclusion of this article will be made available by the authors, without undue reservation.

AUTHOR CONTRIBUTIONS

Conceptualization: SW, YX, and FW; methodology: SW, ZX, and YZ; formal analysis: SW, WW, ZQ, KL, GZ, and FZ; investigation: SW, ZQ, KL, and GZ; data curation: SW, ZX, ZQ, GZ, and FZ; software: ZX, YZ, KL, and FZ; writing—original draft: SW; writing—review and editing: YX; and supervision: FW, WW, and YX.

FUNDING

This research was funded by the Natural Science Foundation of China (Grant Number 42007183), the Fundamental Research Funds for the Central Universities (Grant Number 2682021ZTPY063), the Key Lab of Geo-Environment of Qinghai Province (Grant Number 2021KJ011, 2021KJ00102), the Student Research Training Program of Southwest Jiaotong University (Grant Number 210815), and the Research Project on Teaching Reform of Southwest Jiaotong University (Grant Number 20201023-04).

ACKNOWLEDGMENTS

The authors appreciate the editors and reviewers for their critical comments and suggestions which greatly helped them to improve the present manuscript.

REFERENCES

Banadkooki, F. B., Ehteram, M., Panahi, F., Sh. Sammen, S. S., Othman, F. B., and El-Shafie, A. (2020). Estimation of Total Dissolved Solids (TDS) Using New Hybrid Machine Learning Models. *J. Hydrol.* 587, 124989. doi:10.1016/j.jhydrol.2020.124989

Barbieri, M., Barberio, M. D., Banzato, F., Billi, A., Boschetti, T., Franchini, S., et al. (2021). Climate Change and its Effect on Groundwater Quality. *Environ. Geochem. Health*. doi:10.1007/s10653-021-01140-5

Chaudhry, A. K., and Sachdeva, P. (2020). Groundwater Quality and Non-carcinogenic Health Risk Assessment of Nitrate in the Semi-arid Region of Punjab, India. *J. Water Health* 18 (6), 1073–1083. doi:10.2166/wh.2020.121

Chen, J., Kuang, X., Lancia, M., Yao, Y., and Zheng, C. (2021). Analysis of the Groundwater Flow System in a High-Altitude Headwater Region under Rapid Climate Warming: Lhasa River Basin, Tibetan Plateau. *J. Hydrol. Reg. Stud.* 36, 100871. doi:10.1016/j.ejrh.2021.100871

Díaz-Alcaide, S., and Martínez-Santos, P. (2019). Review: Advances in Groundwater Potential Mapping. *Hydrogeology J.* 27 (7), 2307–2324. doi:10.1111/j.1753-318X.2009.01025.x

Dragon, K. (2021). Identification of Groundwater Conditions in the Recharge Zone of Regionally Extended Aquifer System with Use of Water Chemistry and Isotopes (Lwowek Region, Poland). *J. Hydrol. Reg. Stud.* 34, 100787. doi:10.1016/j.ejrh.2021.100787

Eslami, F., Yaghmaeian, K., Mohammadi, A., Salari, M., and Faraji, M. (2019). An Integrated Evaluation of Groundwater Quality Using Drinking Water Quality Indices and Hydrochemical Characteristics: a Case Study in Jiroft, Iran. *Environ. Earth Sci.* 78 (10), 314. doi:10.1007/s12665-019-8321-1

GAQS (2017). *Standards for Groundwater Quality (GB/T 14848-2017)*. Beijing: General Administration of Quality Supervision.

Gu, X., Xiao, Y., Yin, S., Hao, Q., Liu, H., Hao, Z., et al. (2018). Hydrogeochemical Characterization and Quality Assessment of Groundwater in a Long-Term Reclaimed Water Irrigation Area, North China Plain. *Water* 10 (9), 1209. doi:10.3390/w10091209

Gu, X., Xiao, Y., Yin, S., Liu, H., Men, B., Hao, Z., et al. (2019). Impact of Long-Term Reclaimed Water Irrigation on the Distribution of Potentially Toxic Elements in Soil: An *In-Situ* Experiment Study in the North China Plain. *Ijerph* 16 (4), 649. doi:10.3390/ijerph16040649

Gu, X., Xiao, Y., Yin, S., Pan, X., Niu, Y., Shao, J., et al. (2017a). Natural and Anthropogenic Factors Affecting the Shallow Groundwater Quality in a Typical Irrigation Area with Reclaimed Water, North China Plain. *Environ. Monit. Assess.* 189 (10). doi:10.1007/s10661-017-6229-3

Gu, X., Xiao, Y., Yin, S., Shao, J., Pan, X., Niu, Y., et al. (2017b). Groundwater Level Response to Hydrogeological Factors in a Semi-arid basin of Beijing, China. *J. Water Supply Res. Tec* 66 (4), 266–278. doi:10.2166/aqua.2017.093

Guo, L., Wang, G., Sheng, Y., Shi, Z., and Sun, X. (2019). Groundwater Microbial Communities and Their Connection to Hydrochemical Environment in

Golmud, Northwest China. *Sci. Total Environ.* 695, 133848. doi:10.1016/j.scitotenv.2019.133848

Guo, Y., Li, P., He, X., and Wang, L. (2022). Groundwater Quality in and Around a Landfill in Northwest China: Characteristic Pollutant Identification, Health Risk Assessment, and Controlling Factor Analysis. *Expo. Health*. doi:10.1007/s12403-022-00464-6

Hao, Q., Lu, C., Zhu, Y., Xiao, Y., and Gu, X. (2018). Numerical Investigation into the Evolution of Groundwater Flow and Solute Transport in the Eastern Qaidam Basin since the Last Glacial Period.*Geofluids* 2018. 1–12. doi:10.1155/2018/9260604

Hao, Q., Shao, J., Cui, Y., and Xie, Z. (2014). Applicability of Artificial Recharge of Groundwater in the Yongding River Alluvial Fan in Beijing through Numerical Simulation. *J. Earth Sci.* 25 (3), 575–586. doi:10.1007/s12583-014-0442-6

Hao, Q., Xiao, Y., Chen, K., Zhu, Y., and Li, J. (2020). Comprehensive Understanding of Groundwater Geochemistry and Suitability for Sustainable Drinking Purposes in Confined Aquifers of the Wuyi Region, Central North China Plain. *Water* 12 (11), 3052. doi:10.3390/w12113052

Havril, T., Tóth, Á., Molson, J. W., Galsa, A., and Mádl-Szőnyi, J. (2018). Impacts of Predicted Climate Change on Groundwater Flow Systems: Can Wetlands Disappear Due to Recharge Reduction? *J. Hydrol.* 563, 1169–1180. doi:10.1016/j.jhydrol.2017.09.020

Helena, B., Pardo, R., Vega, M., Barrado, E., Fernandez, J. M., and Fernandez, L. (2000). Temporal Evolution of Groundwater Composition in an Alluvial Aquifer (Pisuerga River, Spain) by Principal Component Analysis. *Water Res.* 34 (3), 807–816. doi:10.1016/s0043-1354(99)00225-0

Huang, L., Wang, L., Zhang, Y., Xing, L., Hao, Q., Xiao, Y., et al. (2018). Identification of Groundwater Pollution Sources by a SCE-UA Algorithm-Based Simulation/Optimization Model. *Water* 10 (2), 193. doi:10.3390/w10020193

Jiang, W., Liu, H., Sheng, Y., Ma, Z., Zhang, J., Liu, F., et al. (2022). Distribution, Source Apportionment, and Health Risk Assessment of Heavy Metals in Groundwater in a Multi-mineral Resource Area, North China. *Expo. Health*. doi:10.1007/s12403-021-00455-z

Li, C., Gao, X., Li, S., and Bundschuh, J. (2020). A Review of the Distribution, Sources, Genesis, and Environmental Concerns of Salinity in Groundwater. *Environ. Sci. Pollut. Res.* 27 (33), 41157–41174. doi:10.1007/s11356-020-10354-6

Li, P., Karunanidhi, D., Subramani, T., and Srinivasamoorthy, K. (2021). Sources and Consequences of Groundwater Contamination. *Arch. Environ. Contam. Toxicol.* 80 (1), 1–10. doi:10.1007/s00244-020-00805-z

Luo, Y., Xiao, Y., Hao, Q., Zhang, Y., Zhao, Z., Wang, S., et al. (2021). Groundwater Geochemical Signatures and Implication for Sustainable Development in a Typical Endorheic Watershed on Tibetan Plateau. *Environ. Sci. Pollut. Res.* 28 (35), 48312–48329. doi:10.1007/s11356-021-14018-x

Ma, R., Zhang, B., and Zhou, X. (2019). The Effects of Climate Change and Groundwater Exploitation on the Spatial and Temporal Variations of Heavy Metal Content in maize in the Luan River Catchment of China. *Environ. Sci. Pollut. Res.* 27 (1), 1035–1052. doi:10.1007/s11356-019-07012-x

Omar, P. J., Gaur, S., Dwivedi, S. B., and Dikshit, P. K. S. (2020). A Modular Three-Dimensional Scenario-Based Numerical Modelling of Groundwater Flow. *Water Resour. Manage.* 34 (6), 1913–1932. doi:10.1007/s11269-020-02538-z

Qu, S., Shi, Z., Liang, X., Wang, G., and Jin, X. (2021). Origin and Controlling Factors of Groundwater Chemistry and Quality in the Zhiluo Aquifer System of Northern Ordos Basin, China. *Environ. Earth Sci.* 80 (12), 439. doi:10.1007/s12665-021-09735-y

Satheeskumar, V., Subramani, T., Lakshumanan, C., Roy, P. D., and Karunanidhi, D. (2020). Groundwater Chemistry and Demarcation of Seawater Intrusion Zones in the Thamirabarani delta of South India Based on Geochemical Signatures. *Environ. Geochem. Health* 43, 757–770. doi:10.1007/s10653-020-00536-z

Sheng, Y., Wang, G., Zhao, D., Hao, C., Liu, C., Cui, L., et al. (2018). Groundwater Microbial Communities along a Generalized Flowpath in Nomhon Area, Qaidam Basin, China. *Groundwater* 56 (5), 719–731. doi:10.1111/gwat.12615

Singh, K. K., Tewari, G., and Kumar, S. (2020). Evaluation of Groundwater Quality for Suitability of Irrigation Purposes: A Case Study in the Udham Singh Nagar, Uttarakhand. *J. Chem.* 2020, 1–15. doi:10.1155/2020/6924026

Su, H., Geng, D., Zhang, Z., Luo, Q., and Wang, J. (2020). Assessment of the Impact of Natural and Anthropogenic Activities on the Groundwater Chemistry in Baotou City (North China) Using Geochemical Equilibrium and Multivariate Statistical Techniques. *Environ. Sci. Pollut. Res.* 27 (22), 27651–27662. doi:10.1007/s11356-020-09117-0

Sun, Q., Shao, J., Wang, Y., and Ma, T. (2019). Research on Appropriate Borehole Density for Establishing Reliable Geological Model Based on Quantitative Uncertainty Analysis. *Arab J. Geosci.* 12 (13), 410. doi:10.1007/s12517-019-4533-7

Venkatramanan, S., Chung, S. Y., Selvam, S., Lee, S. Y., and Elzain, H. E. (2017). Factors Controlling Groundwater Quality in the Yeonjegu District of Busan City, Korea, Using the Hydrogeochemical Processes and Fuzzy GIS. *Environ. Sci. Pollut. Res.* 24 (30), 23679–23693. doi:10.1007/s11356-017-9990-5

WHO (2017). *Guidelines for Drinking-Water Quality Fourth Edition Incorporating the First Addendum*. Geneva, Switzerland: World Health Organization.

Wu, X., Zhang, L., Hu, B. X., Wang, Y., and Xu, Z. (2020). Isotopic and Hydrochemical Evidence for the Salinity Origin in the Coastal Aquifers of the Pearl River Delta, Guangzhou, China. *J. Contaminant Hydrol.* 235, 103732. doi:10.1016/j.jconhyd.2020.103732

Xiao, Y., Hao, Q., Zhang, Y., Zhu, Y., Yin, S., Qin, L., et al. (2022a). Investigating Sources, Driving Forces and Potential Health Risks of Nitrate and Fluoride in Groundwater of a Typical Alluvial Fan plain. *Sci. Total Environ.* 802, 149909. doi:10.1016/j.scitotenv.2021.149909

Xiao, Y., Liu, K., Hao, Q., Li, Y., Xiao, D., and Zhang, Y. (2022b). Occurrence, Controlling Factors and Health Hazards of Fluoride-Enriched Groundwater in the Lower Flood plain of Yellow River, Northern China. *Expo. Health* 14, 2. doi:10.1007/s12403-021-00452-2

Xiao, Y., Liu, K., Hao, Q., Xiao, D., Zhu, Y., Yin, S., et al. (2022c). Hydrogeochemical Insights into the Signatures, Genesis and Sustainable Perspective of Nitrate Enriched Groundwater in the piedmont of Hutuo Watershed, China. *CATENA* 212, 106020. doi:10.1016/j.catena.2022.106020

Xiao, Y., Liu, K., Yan, H., Zhou, B., Huang, X., Hao, Q., et al. (2021a). Hydrogeochemical Constraints on Groundwater Resource Sustainable Development in the Arid Golmud Alluvial Fan plain on Tibetan Plateau. *Environ. Earth Sci.* 80 (22), 750. doi:10.1007/s12665-021-10076-z

Xiao, Y., Shao, J., Cui, Y., Zhang, G., and Zhang, Q. (2017). Groundwater Circulation and Hydrogeochemical Evolution in Nomhon of Qaidam Basin, Northwest China. *J. Earth Syst. Sci.* 126 (2), 8. doi:10.1007/s12040-017-0800-8

Xiao, Y., Shao, J., Frape, S. K., Cui, Y., Dang, X., Wang, S., et al. (2018). Groundwater Origin, Flow Regime and Geochemical Evolution in Arid Endorheic Watersheds: a Case Study from the Qaidam Basin, Northwestern China. *Hydrol. Earth Syst. Sci.* 22 (8), 4381–4400. doi:10.5194/hess-22-4381-2018

Xiao, Y., Xiao, D., Hao, Q., Liu, K., Wang, R., Huang, X., et al. (2021b). Accessible Phreatic Groundwater Resources in the Central Shijiazhuang of North China Plain: Perspective from the Hydrogeochemical Constraints. *Front. Environ. Sci.* 9. doi:10.3389/fenvs.2021.747097

Xiao, Y., Yin, S., Hao, Q., Gu, X., Pei, Q., and Zhang, Y. (2020). Hydrogeochemical Appraisal of Groundwater Quality and Health Risk in a Near-Suburb Area of North China. *J. Water Supply: Res. Technology-Aqua* 69 (1), 55–69. doi:10.2166/aqua.2019.101

Yang, N., Wang, G., Shi, Z., Zhao, D., Jiang, W., Guo, L., et al. (2018). Application of Multiple Approaches to Investigate the Hydrochemistry Evolution of Groundwater in an Arid Region: Nomhon, Northwestern China. *Water* 10 (11), 1667. doi:10.3390/w10111667

Yin, S., Gu, X., Xiao, Y., Wu, W., Pan, X., Shao, J., et al. (2017). Geostatistics-based Spatial Variation Characteristics of Groundwater Levels in a Wastewater Irrigation Area, Northern China. *Water Supply* 17 (5), 1479–1489. doi:10.2166/ws.2017.052

Yin, S., Xiao, Y., Gu, X., Hao, Q., Liu, H., Hao, Z., et al. (2019). Geostatistical Analysis of Hydrochemical Variations and Nitrate Pollution Causes of Groundwater in an Alluvial Fan plain. *Acta Geophys.* 67 (4), 1191–1203. doi:10.1007/s11600-019-00302-5

Yin, S., Xiao, Y., Han, P., Hao, Q., Gu, X., Men, B., et al. (2020). Investigation of Groundwater Contamination and Health Implications in a Typical Semiarid Basin of North China. *Water* 12 (4), 1137. doi:10.3390/w12041137

Yousefi, M., Asghari, F., Zuccarello, P., Oliveri Conti, G., Ejlali, A., Mohammadi, A., et al. (2019). Spatial Distribution Variation and Probabilistic Risk Assessment of Exposure to Fluoride in Ground Water Supplies: A Case

Study in an Endemic Fluorosis Region of Northwest Iran. *Ijerph* 16 (4), 564. doi:10.3390/ijerph16040564

Yousefi, M., Ghoochani, M., and Hossein Mahvi, A. (2018). Health Risk Assessment to Fluoride in Drinking Water of Rural Residents Living in the Poldasht City, Northwest of Iran. *Ecotoxicology Environ. Saf.* 148, 426–430. doi:10.1016/j.ecoenv.2017.10.057

Zhang, J., Jing, H., Dong, K., Jin, Z., and Ma, J. (2022a). The Effect of Drip Irrigation under Mulch on Groundwater Infiltration and Recharge in a Semi-arid Agricultural Region in China. *Water Supply*. doi:10.2166/ws.2022.033

Zhang, L., Li, P., and He, X. (2022b). Interactions between Surface Water and Groundwater in Selected Tributaries of the Wei River (China) Revealed by Hydrochemistry and Stable Isotopes. *Hum. Ecol. Risk Assess. Int. J.* 28 (1), 1–21. doi:10.1080/10807039.2021.2016054

Zhang, Q., Xu, P., Chen, J., Qian, H., Qu, W., and Liu, R. (2021a). Evaluation of Groundwater Quality Using an Integrated Approach of Set Pair Analysis and Variable Fuzzy Improved Model with Binary Semantic Analysis: A Case Study in Jiaokou Irrigation District, East of Guanzhong Basin, China. *Sci. Total Environ.* 767, 145247. doi:10.1016/j.scitotenv.2021.145247

Zhang, Y., Dai, Y., Wang, Y., Huang, X., Xiao, Y., and Pei, Q. (2021b). Hydrochemistry, Quality and Potential Health Risk Appraisal of Nitrate Enriched Groundwater in the Nanchong Area, Southwestern China. *Sci. Total Environ.* 784, 147186. doi:10.1016/j.scitotenv.2021.147186

Zhang, Y., He, Z., Tian, H., Huang, X., Zhang, Z., Liu, Y., et al. (2021c). Hydrochemistry Appraisal, Quality Assessment and Health Risk Evaluation of Shallow Groundwater in the Mianyang Area of Sichuan Basin, Southwestern China. *Environ. Earth Sci.* 80 (17), 576. doi:10.1007/s12665-021-09894-y

Zhao, D., Wang, G., Liao, F., Yang, N., Jiang, W., Guo, L., et al. (2018). Groundwater-surface Water Interactions Derived by Hydrochemical and Isotopic (222Rn, Deuterium, Oxygen-18) Tracers in the Nomhon Area, Qaidam Basin, NW China. *J. Hydrol.* 565, 650–661. doi:10.1016/j.jhydrol.2018.08.066

Conflict of Interest: The authors declare that the research was conducted in the absence of any commercial or financial relationships that could be construed as a potential conflict of interest.

Publisher's Note: All claims expressed in this article are solely those of the authors and do not necessarily represent those of their affiliated organizations, or those of the publisher, the editors, and the reviewers. Any product that may be evaluated in this article, or claim that may be made by its manufacturer, is not guaranteed or endorsed by the publisher.